Nonlinear Analysis of Rotor-AMB System with Current Saturation Effect

Xiaoshen Zhang [1,2,3], Tianpeng Fan [1,2,3], Zhe Sun [*1,2,3], Lei Zhao [1,2,3], Xunshi Yan [1,2,3], Jingjing Zhao [1,2,3], and Zhengang Shi [1,2,3]

[1] Institute of Nuclear and New Energy Technology
[2] Collaborative Innovation Center of Advanced Nuclear Energy Technology
[3] Key Laboratory of Advanced Reactor Engineering and Safety of Ministry of Education
Tsinghua University, Beijing, 100084, China
zxs16@mails.tsinghua.edu.cn, sun_zhe@mail.tsinghua.edu.cn*

Abstract ― The analysis on nonlinear dynamics of a rotor-AMB system is conducted in this paper. The nonlinearity of electromagnetic force and current saturation effect are taken into account. The nonlinear model of the rotor-AMB system is built and the nonlinear dynamic behaviors of the system in both resonance region and non-resonance region are investigated through numerical integration method. This paper shows that the rotor-AMB system can exhibit some complicated nonlinear dynamic behaviors, such as soft spring characteristic of the amplitude-frequency response curve, the jump phenomenon, and pitchfork bifurcation. And the effects of exciting force and current saturation on these nonlinear dynamic behaviors of the system are discussed.

Index Terms ― Current saturation, nonlinear analysis, numerical integration, pitchfork bifurcation.

I. INTRODUCTION

As a typical mechatronic product, active magnetic bearings (AMBs) can achieve the suspension support of the rotor through the electromagnetic forces. An AMB system consists of sensors, controllers, power amplifiers, and mechanical components. The rotor displacement is adjusted by the cooperation of these components. During operation, as the rotor deviates from the reference position, the displacement is measured by the sensor, then measurement signal is transformed into a control signal through the calculation of the controller, which is imported into the power amplifier hereafter. Based on the control signal, the power amplifier exports the control current which will play a key role in magnetic bearings to generate appropriate electromagnetic force to suspend the rotor. Compared with conventional bearings, AMBs have a lot of advantages, such as no mechanical friction between rotor and stator, no wear, lubrication free, long operation life with low maintenance cost, etc. What is more, dynamic characteristics of the rotor can be controlled through the AMBs during system operation. Due to these advantages, AMBs have been widely applied in high-speed rotating machinery, especially those working in special environments.

The modeling, dynamics analysis, and controller design of the rotor-AMBs system were usually based on linearized models which described the characteristics of the system approximately in the linear region near to static levitation position [1], and system identifications were also based on the linearized models [2,3]. The linearized model can meet the research needs of vibration modal analysis and controller design under the condition of small rotor displacements. However, the rotor-AMB systems are substantially nonlinear. The electromagnetic force is a nonlinear function of currents and rotor displacement, and there may exist hysteresis, voltage saturation, and current saturation effects in the system. With the increasing of rotating speed and more extensive use of new structures and materials, the nonlinearities of the rotor-AMB system have become increasingly prominent. Thus the system may exhibit many complicated nonlinear phenomena, such as jump phenomenon, co-existence of multiple solutions, sensitivity to initial conditions, bifurcations and even chaos [4]. The dynamic characteristics of the rotor-AMBs systems are so complicated that linear models could not predict the dynamic behaviors and the stability of the system accurately under various operating conditions [5]. Therefore, it is essential to carry out the nonlinear dynamics analysis of the rotor-AMBs system.

There have been extensive publications about nonlinear characteristics of rotor-bearing systems. For example, Refs. [6,7] investigated the nonlinear dynamics of rotor-film bearing systems and got some valuable results, which were heuristic for the nonlinear dynamics analysis of rotor-AMB systems. However, rotor-AMB systems have some special nonlinear factors because of features of the AMBs, such as the delay of control force [8,9], current, voltage and magnetic saturation [10], and time-varying stiffness [11].

The nonlinear phenomena of rotor-AMB systems have been the focuses of researchers. Many analysis

Submitted On: June 28, 2018
Accepted On: September 24, 2018

methods have been developed and many interesting results have been found. Nonlinear analysis methods applied to rotor-AMB systems can be divided into two categories, namely numerical methods and analytical methods. References [12-14] analyzed the bifurcations of a flexible rotor supported by AMBs numerically. The dynamic behaviors of the system under different operating conditions were studied using the trajectory diagrams, bifurcation diagrams, power spectra and Poincaré maps in [12]. The effects of the system parameters on dynamic characteristics were analyzed and the key factors affecting system performance were identified and demonstrated. References [13,14] investigated the nonlinear dynamic responses of the flexible rotor-AMBs system numerically and proved that nonlinear phenomena such as period-doubling motion, quasi-periodic motion, and even chaotic motion might appear. Moreover, the approximate analytical methods including harmonic balance method, asymptotic perturbation method [15], the method of multiple scales [4], and KBM method [16,17], have been applied widely in nonlinear analysis of rotor-AMB systems. The nonlinear oscillations of a rigid rotor-AMB system taking the time delay into account were studied using the approximate analytical method in [18], and the effects of system parameters on the dynamic behaviors were analyzed. Reference [4] applied the method of multiple scales to obtain an analytical approximate solution of a rotor-AMB system subjected to primary resonance excitations in the presence of 1:1 internal resonance. Based on the analytical approximate solution, a verity of nonlinear phenomena were studied and the analysis results were validated by numerical simulation. References [15,19] utilized the asymptotic perturbation method and the method of multiple scales respectively to investigate the responses of the rotor-AMB system with periodic time-varying stiffness and the system exhibited some typical nonlinear phenomena. References [16,17] utilized KBM method to investigate the nonlinear dynamics of the rotor-bearing system with hysteretic characteristics.

These aforementioned reports about the nonlinear analysis of rotor-AMB systems focused on rotor vibration amplitudes, which will have a significant effect on system stability. However, the rotor-AMB system has a larger air gap between the rotor and stator than rotor systems supported by conventional bearings due to the non-contact suspension support feature. Under certain operating conditions, the nonlinear rotor-AMB system may have multiple equilibrium solutions, namely, the rotor may vibrate in different equilibrium positions. In this case, the rotor's maximal instantaneous displacement is dependent on both rotor equilibrium position and vibration amplitude. And if rotor displacement is large, the rotor-AMB system may lose its stability. Therefore, equilibrium solutions also have an important influence on system stability as well as the vibration amplitude. There were few reports about rotor equilibrium positions of the rotor-AMB system. Nevertheless, the rotor-AMB system is expected to operate in non-resonance regions, where the rotor doesn't exhibit complicated characteristics in vibration amplitude generally. Whereas there may exist some other nonlinear phenomena in non-resonance regions, which also have effect on the system performance but didn't attract enough attention. For example, the pitchfork bifurcation phenomenon was discovered in site-commissioning of a rotor-AMB system with current saturation effect, which meant that new equilibrium solutions occurred in the system. It was detrimental to system performance.

In this paper, a single-degree-of-freedom rotor-AMB system with current saturation effect is investigated through numerical integration method. The nonlinear model of the rotor-AMB system considering current saturation effect is deduced firstly. Then the amplitude-frequency response characteristics and rotor dynamic behaviors in the non-resonance region are analyzed numerically based on the system differential equation of motion. The system exhibits soft-spring characteristics, jump phenomena, and pitchfork bifurcation. The effects of exciting force and current saturation on system dynamic behaviors are illustrated and controller parameter modification is conducted. This paper concentrates on nonlinear phenomena of the rotor-AMB system in both non-resonance and resonance regions, which extends the nonlinear dynamic analysis of the rotor-AMB system to full speed range and enriches the nonlinear dynamic theory of the rotor-AMB system. The investigation of pitchfork bifurcation in non-resonance can supply the research gap in nonlinear analysis of the rotor-AMB system and help to understand the system's nonlinear dynamics in the round. And through the comprehensive nonlinear dynamics analysis of the system with current saturation, the nonlinear dynamic behaviors are illustrated in detail and the causes of the nonlinear phenomenon are explored in depth. The analysis result can play an important role in the efforts to improve system performance. For example, the controller adjustment based on nonlinear analysis results can achieve the goal of improving system performance that the efforts based on linear analysis couldn't do.

II. THEORETICAL MODEL

This paper takes an actual rotor-AMB system as a research object. During commissioning, the system lost its stability and the current saturation phenomenon was discovered by analyzing the operational data. In order to explore the instability mechanism, the nonlinear model is built and nonlinear analysis through cell mapping method is conducted by authors of this paper [20]. In this paper, the nonlinear dynamics of the rotor-AMB system is investigated using numerical integration method and dynamic behaviors in both resonance and non-resonance

regions are analyzed. Just as Ref. [20], the rotor-AMB system is simplified into a single-degree-of-freedom model for simplicity of the analysis in this paper, which focuses on the direction where nonlinear phenomena occur.

A. System model

The diagram of the simplified system model is shown in Fig. 1.

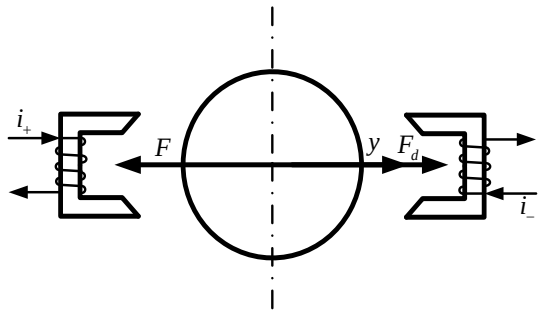

Fig. 1. Schematic diagram of single-degree-of-freedom rotor-active magnetic bearings system.

Where, y represents the displacement of the rotor, i_+, i_- represents the currents from the power amplifier to the magnets respectively, F represents the electromagnetic force, and F_d represents the exciting force. The exciting force is assumed to be sinusoidal, as shown in equation (1):

$$F_d = |F_d|\cos(\Omega t). \tag{1}$$

The open-loop system is inherently unstable. For the analyzing the dynamic characteristics of the system, a PD controller is adopted to keep the system stable. The magnetic hysteresis and fringing effect are not taken into account. The sensor is taken as a proportional component whose gain is k. And a current-type power amplifier is employed in the system, in which the current saturation is taken into account. The closed-loop diagram of the system is shown in Fig. 2.

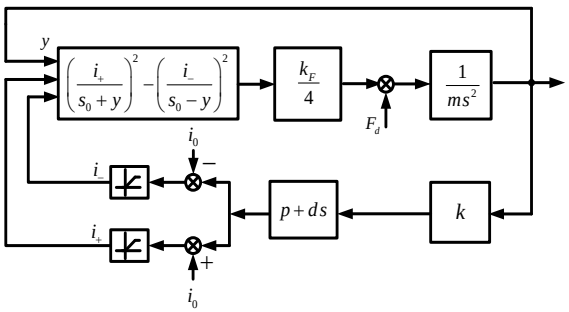

Fig. 2. Closed-Loop Diagram of Rotor-AMB System.

In the actual system, the currents in the power amplifier are limited to a certain range. Thus, the currents of the two magnets, namely, i_+, i_-, can be expressed as a piecewise function shown in equation (2):

$$\begin{aligned} i_+ &= \mathrm{med}(0, i_0+i, i_m) = \begin{cases} 0 & i_0+i<0 \\ i_0+i & 0\le i_0+i\le i_m \\ i_m & i_m\le i_0+i \end{cases}, \\ i_- &= \mathrm{med}(0, i_0-i, i_m) = \begin{cases} 0 & i_0-i<0 \\ i_0-i & 0\le i_0-i\le i_m \\ i_m & i_m\le i_0-i \end{cases}, \\ i &= k(py+d\dot{y}), \end{aligned} \tag{2}$$

where, i_0 represents the bias current of the magnetic bearing and i represents the control current, $\dot{y}$ represents the first order derivative of rotor displacement, and 'med' means the median value of the three values in the bracket.

In the rotor-AMB systems, the electromagnetic force is a nonlinear function of the rotor displacement and the currents in magnetic bearings. The electromagnetic force model in Ref. [1] is adopted and can be formulated as equation (3):

$$F = \frac{1}{4}k_F\left(\left(\frac{i_+}{s_0+y}\right)^2-\left(\frac{i_-}{s_0-y}\right)^2\right), \tag{3}$$

where, s_0 is the air gap of the bearing at the reference position, and k_F is the force coefficient related to the system. It can be seen from equation (3) that the existence of the current saturation makes nonlinear characteristics of the system more complicated.

Based on basic laws of the classical mechanics, the governing equation of the closed-loop system shown in Fig. 2 is deduced, as shown in equation (4):

$$\ddot{y} = \frac{1}{m}\left(-F+|F_d|\cos(\Omega t)\right), \tag{4}$$

where m is the mass of the rotor.

Then the mathematical model of the rotor-AMB system is made up of the equations (1), (2), (3), (4).

B. Nondimensionalization

In order to facilitate analysis and obtain the visualized results, the governing equations of the system obtained above are transformed into the dimensionless form by introducing the following dimensionless variables and corresponding notations:

$$\begin{aligned} &y' = \frac{y}{s_0},\ \Omega' = \frac{\Omega}{\Omega_0},\ \tau = \Omega_0 t, \\ &i' = \frac{i}{i_m},\ i_0' = \frac{i_0}{i_m},\ i_\pm' = \frac{i_\pm}{i_m}, \\ &p' = \frac{ps_0}{i_m},\ d' = \frac{\Omega_0 d s_0}{i_m},\ \tilde{k}_F = \frac{k_F}{4}\frac{i_m^2}{\Omega_0{}^2 s_0^3}, \\ &\left|\tilde{F}_d\right| = \frac{1}{\Omega_0{}^2 s_0}|F_d|, \end{aligned} \tag{5}$$

where, Ω_0 is the rated operating speed of the rotor. Substitute equation (5) into equations (1), (2), (3), and (4), then dimensionless form model of the system is obtained, as shown in equation (6):

$$\begin{aligned} i'_{\pm} &= \mathrm{med}\left(0, i'_0 \pm i', 1\right), \\ i' &= k\left(p'y' + d'\frac{\mathrm{d}}{\mathrm{d}\tau}y'\right), \\ \tilde{F} &= \tilde{k}_F\left(\left(\frac{i'_+}{1+y'}\right)^2 - \left(\frac{i'_-}{1-y'}\right)^2\right), \\ \frac{\mathrm{d}^2}{\mathrm{d}\tau^2}y' &= \frac{1}{m}\left(-\tilde{F}\right) + \left|\tilde{F}_d\right|\cos\left(\Omega'\tau\right). \end{aligned} \tag{6}$$

In the non-dimensional model, i'_0=0.5, $k = 45000$, $\tilde{k}_F$=0.0099. In the following, the values of these variables are fixed at these values and other parameters will be assigned.

III. RESULTS AND DISCUSSIONS

Based on the dimensionless form model obtained in the previous section, the nonlinear dynamics of the rotor-AMB system is investigated numerically. In this section, equation (6) is solved to get time series solutions of multiple variables by Runge-Kutta 5(4) algorithm [21] under different conditions. Then the time responses of rotor displacement, currents, and electromagnetic force are obtained. Based on the rotor displacement time series responses, the displacements at chosen Poincaré points of motion periods are gotten by Poincaré map and vibration amplitude *a* is calculated according to equation (7):

$$\begin{aligned} b_1 &= 2\int y'(\tau)\sin\Omega'\tau\,\mathrm{d}\tau, \\ b_2 &= 2\int y'(\tau)\cos\Omega'\tau\,\mathrm{d}\tau, \\ a &= \sqrt{b_1^2 + b_2^2}. \end{aligned} \tag{7}$$

In the following of this section, the amplitude-frequency response of the system is acquired and the pitchfork bifurcation phenomenon is discovered and interpreted. Based on analysis results, the controller parameters are adjusted to avoid pitchfork bifurcation, which has a detrimental effect on system stability.

A. Amplitude-frequency response of system

The amplitude-frequency response is one of the important characteristics of the rotor-AMB system, which play a key role in the system performance analysis and controller design. However, the amplitude-frequency response based on nonlinear model differs from that based on the linear model.

In this subsection, parameters of the PD controller are fixed at $p' = 4.232\times10^{-5}$, $d' = 1.0668\times10^{-4}$. Then amplitude-frequency response curves of the rotor-AMB system for different exciting magnitudes are obtained. When the exciting force's magnitudes are 0.354, 0.4132, 0.4722, the amplitude-frequency response curves are shown in Fig. 3 respectively. In Fig. 3, *a* is the dimensionless vibration amplitude of rotor situated in zero equilibrium position. In this case, the rotor's maximal instantaneous displacement only depends on vibration amplitude and is just the vibration amplitude. It contrasts with that in case of pitchfork bifurcation which will be described in the next subsection.

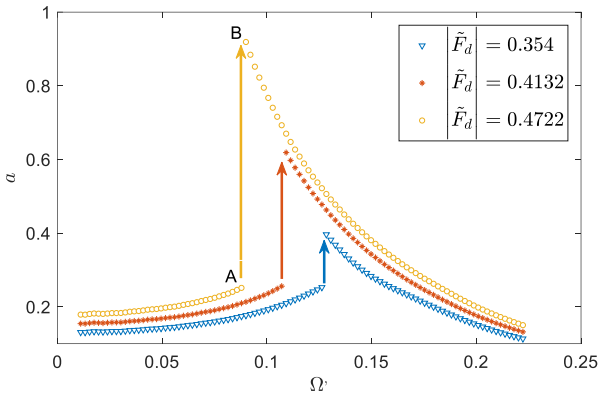

Fig. 3. The amplitude-frequency response of the rotor-AMB system.

It can be seen from Fig. 3 that the vibration amplitude of the rotor is not only dependent on exciting magnitudes, but also related to exciting frequencies. With the increase of exciting force, the vibration amplitude magnifies. Meanwhile, as the exciting frequency increases, the rotor amplitude first increases and then decreases after some specific frequency where there is a resonance peak. This result is consistent with that based on the linear system. However, the nonlinear system also exhibits more complicated phenomena, such as soft-spring characteristics and jump phenomenon. As shown in Fig. 3, the frequencies where resonance peaks occur are different for different exciting magnitudes. As the exciting magnitude increases, the resonance peak moves to low-frequency zone, i.e., the resonant frequency becomes smaller. In addition, there is another nonlinear phenomenon in Fig. 3. In the vicinity of resonance peaks, the vibration amplitudes mutate with a slight exciting frequency change. Take $\left|\tilde{F}_d\right|$=0.4722 as an example, the amplitude *a* increases gradually as frequency increases until it reaches the point A. However, at the point A, as frequency increases lightly, the amplitude *a* jumps from the point A to the point B and the rotor vibration amplitude reaches the peak value. Subsequent to that, the amplitude decreases gradually with the increase of exciting frequency. It is a typical jump phenomenon of nonlinear systems. Furthermore, it can be seen in Fig. 3 that, the larger exciting force is, the more obvious the

jump phenomenon and soft-spring characteristics are.

In order to explore the causes of nonlinear phenomena in the resonance region of the rotor-AMB system, the current and electromagnetic force at point B are shown in Fig. 4 and Fig. 5. In Fig. 5, $\tilde{F}_+, \tilde{F}_-$ represent the attractive force generating by the two magnets respectively, which can be formulated as $\tilde{F}_\pm = \tilde{k}_F \left(\frac{i'_\pm}{1 \pm y'} \right)^2$. It can be seen that severe current saturation has occurred and the electromagnetic force acting as restoring force in the system distort. It leads to the soft-spring characteristic and jump phenomenon, which have detrimental influences on the stability of the rotor-AMB system. In brief, the nonlinearity of electromagnetic force and current saturation existing in the system are the causes of complicated dynamic behaviors when the rotor-AMB system is subjected to the exciting force.

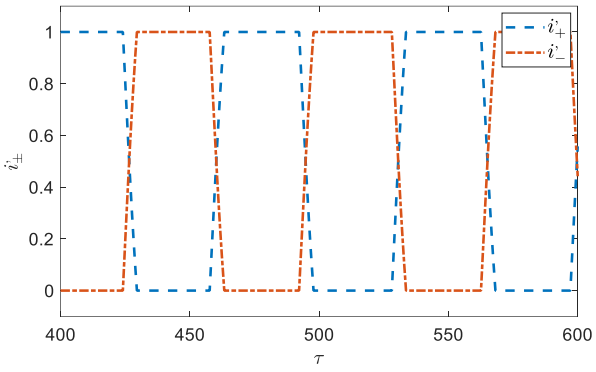

Fig. 4. The partial enlarged detail of current at point B of Fig. 3.

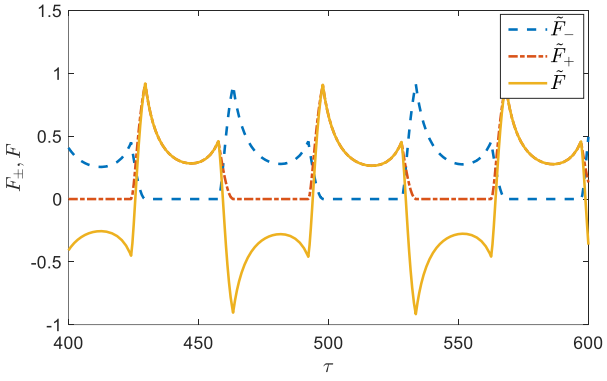

Fig. 5. The partial enlarged detail of electromagnetic force at point B of Fig. 3.

B. Pitchfork bifurcation

When the system is running stably, the rotor speed is generally far from the resonance zone. However, the rotor-AMB system with current saturation effect still exhibits the nonlinear phenomenon when the system is operating in the non-resonance region. In this subsection, the oscillations of the rotor under different initial conditions are investigated and the bifurcation diagram of the rotor versus the exciting force is obtained. The effects of the exciting force and the current saturation in the power amplifier on the vibration of the rotor are also illustrated.

In the analysis, these parameters of the system are fixed at $p' = 4.232\times10^{-5}$, $d' = 1.0668\times10^{-4}$, $\Omega'=1$. Two different initial conditions are respectively set as $[y'_{10} = 0.0536, \dot{y}'_{10} = 0.0093]$, $[y'_{20} = 0.403, \dot{y}'_{20} = 0.0093]$. The dynamic behaviors of the system for different exciting forces are analyzed. The time series responses of the rotor-AMB system subjected to exciting forces under different initial conditions are solved by Runge-Kutta 5(4) method with variable step size. And the rotor displacements at Poinceré map points which are the specific time instants of motion periods are obtained from corresponding time series responses through Poincaré map. Then the bifurcation diagram versus the amplitude of the exciting force is obtained, as shown in Fig. 6. The abscissa of the Fig. 6 is the magnitude of the exciting force, while the ordinate is the displacement at the specific Poincaré map point. Different from that in subsection A, the rotor displacements at Poincaré map points y'_1, y'_2 in Fig. 6 depend on both rotor equilibrium positions and vibration amplitudes. In order to explain the relationship between the rotor displacements at Poincaré map points shown in Fig. 6 and time series response, taking $|\tilde{F}_d| = 16.83$ as an example to point out the correspondence between Fig. 6 and Fig. 10. The displacements shown in Fig. 6 are the mean values of the Poincaré map points' displacements in Fig. 10 after system enters steady state. It is noted that Fig. 10 is the partial enlarged drawing of the time series response and the mapping points shown in Fig. 10 are only part of all mapping points. Because of the chosen mapping points, y'_1 is the maximal instantaneous displacement under corresponding initial condition, while y'_2 is not. But, the maximal instantaneous displacements for two different initial conditions are both the sum of the absolute value of equilibrium positions and vibration amplitude.

It can be seen in Fig. 6 that when the exciting force is small, the amplitudes of the rotor vibration are small and rotor displacements of the Poincaré map points for different initial conditions are consistent, i.e., both rotor equilibrium positions and vibration amplitudes for two different initial conditions are the same. The rotor vibrates at zero equilibrium position for small exciting force and with the increase of the exciting force, the vibration amplitude tends to be larger. In case of small exciting forces, the responses of the rotor-AMB system based on the nonlinear model are consistent with those

based on the linearized model and rotor displacements depend only on vibration amplitudes. However, as the exciting force continues to magnify, the pitchfork bifurcation appears in the vicinity of $|\tilde{F}_d| = 16.04$, where rotor displacements for different initial conditions are different. The rotor deviates from zero equilibrium position and vibrates at either of two new different equilibrium positions. This is a typical supercritical pitchfork bifurcation. With further increase of exciting force, the pitchfork bifurcation aggravates. In the case of pitchfork bifurcation, the Poincaré map points' rotor displacements are not only dependent on vibration, but also dependent on rotor vibration positions.

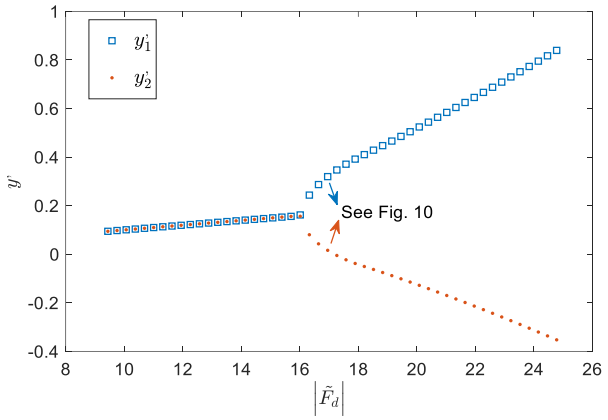

Fig. 6. Pitchfork bifurcation: rotor displacement at Poincaré map points versus exciting magnitude.

In order to understand the bifurcation further and reveal the causes of this phenomenon, two different exciting forces in Fig. 6 are taken as examples to illustrate the influences of the exciting force and current saturation on the dynamic behaviors of the rotor.

For $|\tilde{F}_d| = 9.44$, the pitchfork bifurcation doesn't appear. The system time series responses, currents in the system, and electromagnetic forces are shown in Fig. 7, Fig. 8, and Fig. 9, respectively. It is noted that for the same exciting force, currents and electromagnetic forces in the system for two different initial conditions are the same after the system enters steady state. So this paper just takes the currents and the electromagnetic forces under one initial condition to show the current and electromagnetic force state of the system in Fig. 8 and Fig. 9. And the same drawing way is used below.

Figure 7 shows the dynamic response of the rotor for $|\tilde{F}_d| = 9.44$. It can be seen that as the exciting force is small, the responses of the rotor for two different initial conditions tend to be consistent and rotor vibrates periodically with the same constant amplitude at the zero equilibrium position. According to Fig. 8 and Fig. 9, the current saturation doesn't occur and electromagnetic force generated by the current is sinusoidal as expected. In a word, as the exciting force is sufficiently small, the system can generate sufficient currents and electromagnetic force to keep rotor vibrating at zero equilibrium position. And the rotor's maximal instantaneous displacements are the rotor vibration amplitudes. It can be seen from Fig. 7 that rotor displacements are small during operation.

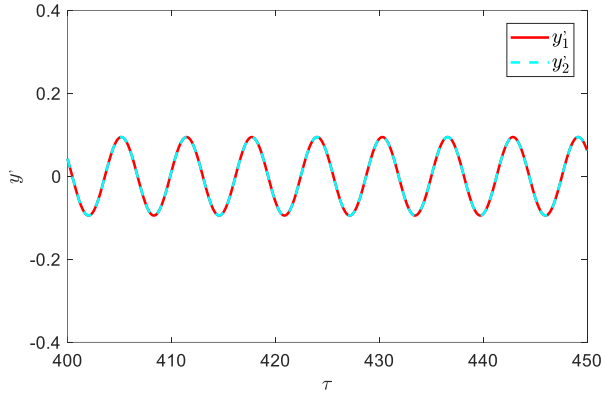

Fig. 7. The partial enlarged detail of system time series responses for $|\tilde{F}_d| = 9.44$.

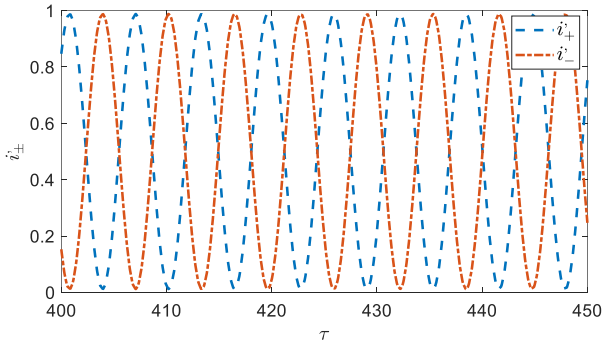

Fig. 8. The partial enlarged detail of currents for $|\tilde{F}_d| = 9.44$.

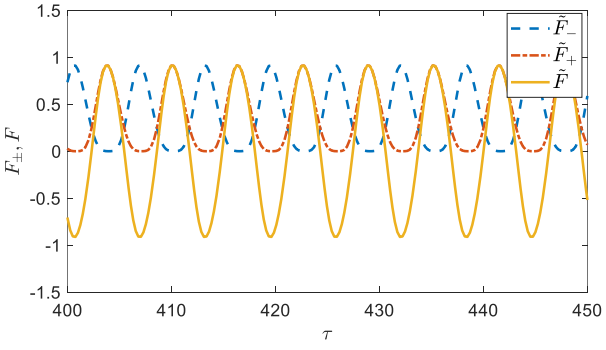

Fig. 9. The partial enlarged detail of electromagnetic force for $|\tilde{F}_d| = 9.44$.

However, as the exciting force becomes larger, the bifurcation appears. For $\left|\tilde{F}_d\right|=16.83$, the system time series response, currents in the system, and electromagnetic force are shown in Fig. 10, Fig. 11, and Fig. 12, respectively.

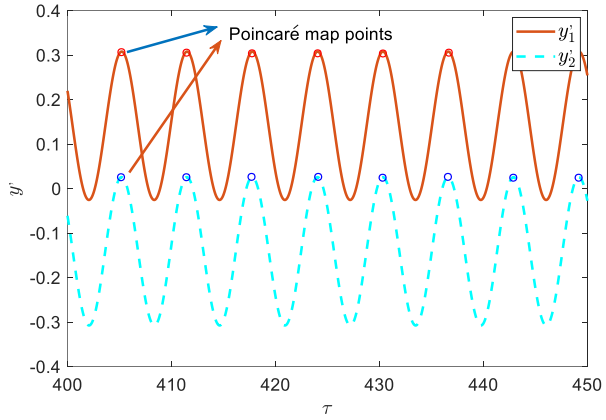

Fig. 10. The partial enlarged detail of system time series responses for $\left|\tilde{F}_d\right|=16.83$.

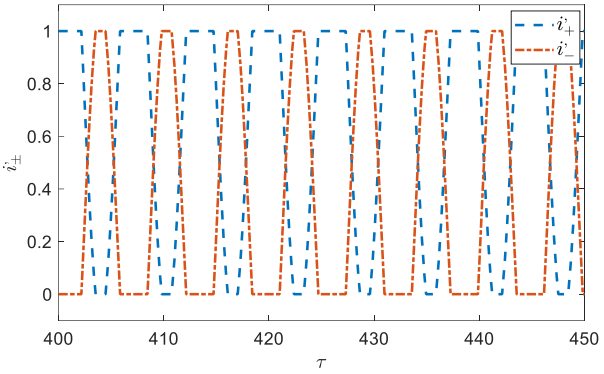

Fig. 11. The partial enlarged detail of current for $\left|\tilde{F}_d\right|=16.83$.

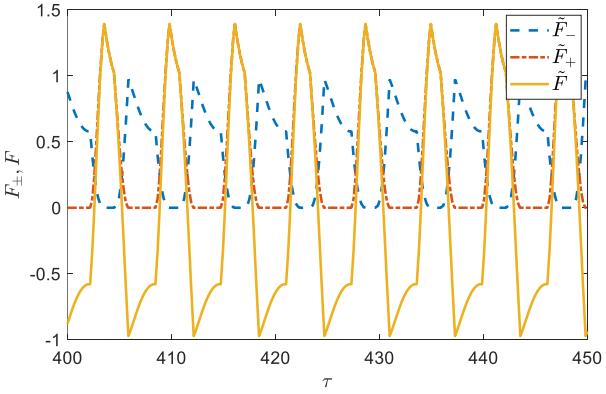

Fig. 12. The partial enlarged detail of electromagnetic force for $\left|\tilde{F}_d\right|=16.83$.

It can be seen from Fig. 10 that system time series responses for slightly different initial conditions are very different for $\left|\tilde{F}_d\right|=16.83$. The rotor may vibrate at different positions deviating from the zero equilibrium position and the new possible equilibrium positions are symmetrical about the original equilibrium position. Figure 11 shows conspicuous current saturation has occurred. And the electromagnetic force shown in Fig. 12 has distorted seriously. In case of current saturation, as the exciting force continues to magnify, the vibration amplitude of the rotor tends to increase, and the needed restoring force calculated by the controller is larger. That means the current in the magnetic bearings should have continued to magnify. However, the existence of the current saturation has limited the increase of the electromagnetic force. At zero equilibrium position, the electromagnetic force contributed by the currents and displacement of the rotor is not enough to suppress the vibration effectively. In order to keep the balanced state, another factor affecting the electromagnetic force, namely the displacement of the rotor, should be larger in the presence of current saturation. Hence, the rotor deviates from the zero equilibrium position to new equilibrium positions. It follows that the sensitivity of the nonlinear system to initial conditions leads to the pitchfork bifurcation.

In this case, the pitchfork bifurcation occurs. The rotor deviates from zero equilibrium position. The rotor's maximal instantaneous displacement is the sum of the absolute value of new equilibrium and vibration amplitude. As Fig. 6, Fig. 7 and Fig. 10 show, the rotor equilibrium position has a prominent effect on the rotor's maximal instantaneous displacement. So, in order to keep rotor-AMB system stable during operation, the equilibrium positions of the system are important as well as vibration amplitudes.

It can be concluded that: as exciting force is small, there is no current saturation in the rotor-AMB system and the zero equilibrium solution exists and is stable. The rotor displacement is only dependent on vibration amplitude. However, with the increase of exciting force, the current saturation occurs gradually and the electromagnetic force generated in the system is not large enough to keep rotor vibrating at zero equilibrium position. The zero equilibrium solution loses its stability and two new equilibrium solutions come up. And it is a typical supercritical pitchfork bifurcation. So, as exciting force is large, the rotor's maximal instantaneous displacement, which has a great effect on the system stability, is dependent on both equilibrium position and vibration amplitude of the rotor-AMB system.

C. Controller parameter modification

According to the analysis results in the previous subsection, the current saturation is the main causes of

pitchfork bifurcation. In this subsection, the controller parameter adjustment is conducted to avoid the current saturation and pitchfork bifurcation phenomenon during system operation.

Through the analysis results in subsection B, it is found that controller parameters can influence the severity of current saturation. The smaller proportional gain p' is, the more serious the current saturation. While the differential gain d' has the opposite effect that the larger differential gain is, the more serious current saturation becomes. As pitchfork bifurcation appears, the rotor's maximal instantaneous displacement becomes larger, which has an adverse effect on system stability. In order to keep the system stable, the bifurcation should be prevented by increasing proportional gain p' and decreasing differential gain d'. In the actual system, the modification of controller parameters is also limited by other factors.

In the next analysis, controller parameters are modified to be $p'=4.461\times10^{-5}$, $d'=4.117\times10^{-5}$ based on the operating condition of the actual system. The change of rotor displacements at Poincaré map points versus exciting magnitude for two different initial conditions is shown in Fig. 13. Compared with Fig. 6, the pitchfork bifurcation disappears after controller parameter modification. The rotor vibrates at the zero equilibrium position for all exciting forces and vibration amplitude tends to be larger with the increase of exciting force. Also take $\left|\tilde{F}_d\right|=16.83$ as an example to show the current and electromagnetic force in this case, as shown in Fig. 14 and Fig. 15, respectively. It can be seen the current saturation doesn't appear and electromagnetic force doesn't distort. These dynamic behaviors of the system prove that modified controller parameters are very effective to avoid the pitchfork bifurcation, which is detrimental to the stability of the rotor-AMB system.

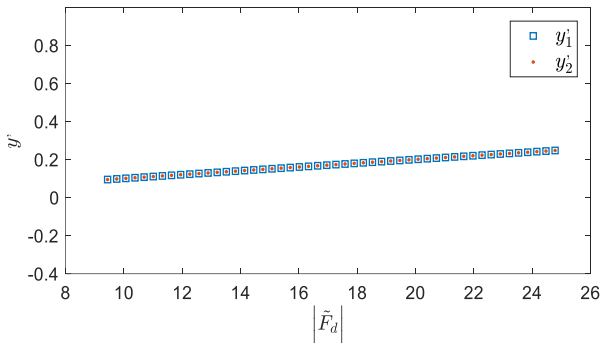

Fig. 13. The rotor displacements at Poincaré map points versus exciting magnitude after controller parameter modification.

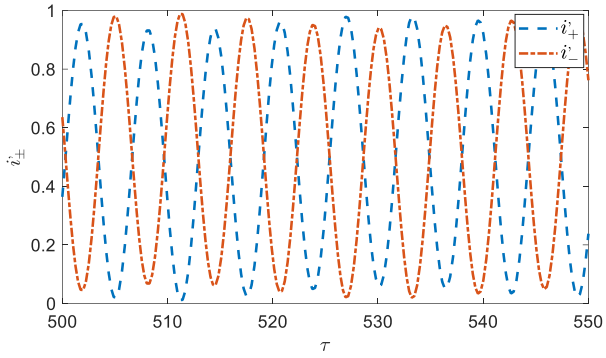

Fig. 14. The partial enlarged detail of current for $\left|\tilde{F}_d\right|=16.83$ after controller parameter modification.

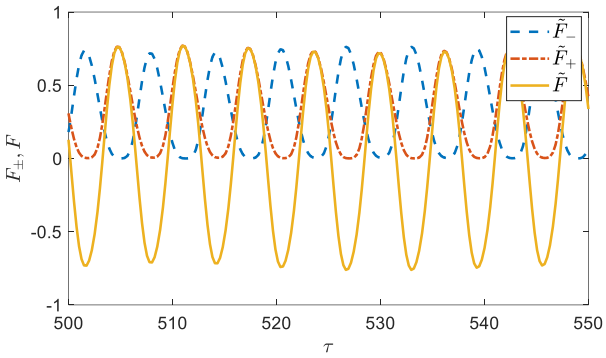

Fig. 15. The partial enlarged detail of electromagnetic force for $\left|\tilde{F}_d\right|=16.83$ after controller parameter modification.

In summary, the large air gap between the rotor and stator provides the possibility of pitchfork bifurcation. And extreme operating conditions, such as heavy load and large disturbance, lead to the phenomenon. The find of pitchfork bifurcation shows that nonlinear dynamic analysis makes sense in full speed range of the rotor-AMB system. And nonlinear phenomena adverse to system performance can be prevented through proper controller adjustment.

IV. CONCLUSIONS AND PROSPECTS

In this paper, the rotor-AMB with a PD controller is investigated numerically and the nonlinearity of electromagnetic force and current saturation effect are taken into account in the analysis. The nonlinear dynamic behaviors of the rotor-AMB system in both resonance and non-resonance regions are analyzed in detail. And the effects of the exciting force and the current saturation on the dynamic behaviors of the rotor-AMB system

are illustrated and the specific controller parameter optimization is conducted based on analysis results. The results reveal that:

(1) There are a soft-spring characteristic and jump phenomenon in the resonance region. Compared with the linear system, the rotor vibration amplitude has a saltation when the rotor passes the resonant frequency.

(2) There is a supercritical pitchfork bifurcation in the non-resonance region. With the increase of exciting force, the zero equilibrium solution loses its stability and two new equilibrium solutions come up. In the case of pitchfork bifurcation, the equilibrium positions and vibration amplitude affects the rotor displacement which has a key effect on the system stability.

(3) The effects of exciting force and current saturation on the nonlinear dynamics are illustrated in detail and optimized controller parameters can suppress the occurrence of bifurcation effectively. So appropriate controller design can prevent complicated nonlinear phenomena and keep the system stable.

The future work of this paper is to apply some special numerical integration methods to investigate the nonlinear dynamic behaviors more precisely [22]. In fact, in this paper, the governing equation is solved by Runge-Kutta 5(4) algorithm. However, the precision of Runge-Kutta 5(4) method is not sufficient in some cases including solving the stiff equations. And in numerical integration, the conservation laws of the mechanical quantities may be infringed. Therefore, some different numerical integration methods should be utilized in nonlinear dynamic analysis of rotor-AMB system.

ACKNOWLEDGMENT

This Paper is financially supported by National Science and Technology Major Project of China (2011ZX069) and Project 61305065 supported by National Natural Science Foundation of China (NSFC).

REFERENCES

[1] G. Schweitzer and E. H. Maslen, *Magnetic Bearings: Theory, Design, and Application to Rotating Machinery*. Springer, 2009.

[2] Z. Sun, J. Zhao, Z. Shi, and S. Yu, "Identification of Flexible Rotor Suspended by Magnetic Bearings," *Proceeding of 21st International Conference on Nuclear Engineering*, 2013.

[3] Z. Sun, Y. He, J. Zhao, Z. Shi, L. Zhao, and S. Yu, "Identification of active magnetic bearing system with a flexible rotor," *Mechanical Systems & Signal Processing*, vol. 49, no. 1-2, pp. 302-316, 2014.

[4] N. A. Saeed, M. Eissa, and W. A. El-Ganini, "Nonlinear oscillations of rotor active magnetic bearings system," *Nonlinear Dynamics*, vol. 74, no. 1-2, pp. 1-20, 2013.

[5] J. Ji and C. H. Hansen, "Non-linear oscillations of a rotor in active magnetic bearings," *Journal of Sound & Vibration*, vol. 240, no. 4, pp. 599-612, 2001.

[6] A. Hu, L. Hou, and L. Xiang, "Dynamic simulation and experimental study of an asymmetric double-disk rotor-bearing system with rub-impact and oil-film instability," *Nonlinear Dynamics*, vol. 84, no. 2, pp. 1-19, 2015.

[7] L. Xiang, X. Gao, and A. Hu, "Nonlinear dynamics of an asymmetric rotor-bearing system with coupling faults of crack and rub-impact under oil-film forces," *Nonlinear Dynamics*, vol. 86, no. 2, pp. 1-11,2016.

[8] T. Inoue, Y. Sugawara, and M. Sugiyama, "Modeling and nonlinear vibration analysis of a rigid rotor system supported by the magnetic bearing (effects of delays of both electric current and magnetic flux)," *Neuroimage*, vol. 13, no. 13, pp. 1203-1203, 2010.

[9] J. Ji, "Stability and Hopf bifurcation of a magnetic bearing system with time delays," *Journal of Sound & Vibration*, vol. 259, no. 4, pp. 845-856, 2013.

[10] K. Kang and A. Palazzolo, "Homopolar magnetic bearing saturation effects on rotating machinery vibration," *IEEE Transactions on Magnetics*, vol. 48, no. 6, pp. 1984-1994, 2012.

[11] W. Zhang and X. Zhan, "Periodic and chaotic motions of a rotor-active magnetic bearing with quadratic and cubic terms and time-varying stiffness," *Nonlinear Dynamics*, vol. 41, no. 4, pp. 331-359, 2005.

[12] M. J. Jang and C. K. Chen, "Bifurcation analysis in flexible rotor supported by active magnetic bearing," *International Journal of Bifurcation & Chaos*, vol. 11, no. 08, pp. 2163-2178, 2001.

[13] J. I. Inayat-Hussain, "Geometric coupling effects on the bifurcations of a flexible rotor response in active magnetic bearings," *Chaos Solitons & Fractals*, vol. 41, no. 5, pp. 2664-2671, 2009.

[14] J. I. Inayat-Hussain, "Nonlinear dynamics of a statically misaligned flexible rotor in active magnetic bearings," *Communications in Nonlinear Science & Numerical Simulation*, vol. 15, no. 3, pp. 764-777, 2010.

[15] W. Zhang, M. Yao, and X. Zhan, "Multi-pulse chaotic motions of a rotor-active magnetic bearing system with time-varying stiffness," *Chaos Solitons & Fractals*, vol. 27, no. 1, pp. 175-186, 2006.

[16] F. Sorge, "Stability analysis of rotor whirl under nonlinear internal friction by a general averaging approach," *Journal of Vibration & Control*, vol. 16, no. 4, pp. 301, 2015.

[17] F. Sorge, "Approach to rotor-shaft hysteretic whirl using Krylov-Bogoliubov techniques," *Journal of Vibration & Control*, vol. 21, no. 5, pp. 883-895, 2013.

[18] T. Inoue, Y. Ishida, and S. Murakami, "Theoretical

analysis and experiments of the nonlinear vibration in a vertical rigid rotor supported by the magnetic bearing system," *Journal of System Design & Dynamics*, vol. 1981, no. 1, pp. 295-306, 2007.

[19] M. Kamel and H. S. Bauomy, "Nonlinear study of a rotor–AMB system under simultaneous primary-internal resonance," *Applied Mathematical Modelling*, vol. 34, no. 10, pp. 2763-2777, 2010.

[20] Z. Sun, X. Zhang, T. Fan, X. Yan, J. Zhao, L. Zhao, and Z. Shi, "Nonlinear dynamic characteristics analysis of active magnetic bearing system based on cell mapping method with a case study," *Mechanical Systems & Signal Processing*, vol. 117, pp. 116-137, 2019.

[21] J. R. Dormand and P. J. Prince, "A family of embedded Runge-Kutta formulae," *Journal of Computational & Applied Mathematics*, vol. 6, no. 1, pp. 19-26, 1980.

[22] B. Leimkuhler and S. Reich, *Simulating Hamiltonian Dynamics*. Cambridge University Press, 2004.

Xiaoshen Zhang (1993.03), Ph.D. candidate of Institute of Nuclear and New Energy Technology, Tsinghua University, Beijing, China. His research interests are the nonlinear dynamics analysis and control of the rotor-AMB system.

Tianpeng Fan (1993.07-) received his Bachelor's degree in Engineering in 2016 from School of Energy Science and Engineering of Harbin Institute of Technology, Harbin. He is studying for a Master's degree in the Institute of Nuclear and New Energy Technology, Tsinghua University. His research interests are unbalance control of rotor and system identification.